AFRL-RX-WP-TP-2008-4327

DIRECT ATOMIC SCALE OBSERVATION OF THE STRUCTURE AND CHEMISTRY OF ORDER/DISORDER INTERFACES (PREPRINT)

R. Srinivasan, R. Banerjee, J.Y. Hwang, G.B. Viswanathan, J. Tiley, and H.L. Fraser

Metals Branch
Metals, Ceramics, and NDE Division

FEBRUARY 2008

AIR FORCE RESEARCH LABORATORY
MATERIALS AND MANUFACTURING DIRECTORATE
WRIGHT-PATTERSON AIR FORCE BASE, OH 45433-7750
AIR FORCE MATERIEL COMMAND
UNITED STATES AIR FORCE

REPORT DOCUMENTATION PAGE

Form Approved
OMB No. 0704-0188

1. REPORT DATE *(DD-MM-YY)*	2. REPORT TYPE	3. DATES COVERED *(From - To)*
February 2008	Journal Article Preprint	

4. TITLE AND SUBTITLE
DIRECT ATOMIC SCALE OBSERVATION OF THE STRUCTURE AND CHEMISTRY OF ORDER/DISORDER INTERFACES (PREPRINT)

5a. CONTRACT NUMBER
In-house

5b. GRANT NUMBER

5c. PROGRAM ELEMENT NUMBER
62102F

6. AUTHOR(S)
R. Srinivasan, G.B. Viswanathan, and H.L. Fraser (The Ohio State University)
R. Banerjee and J.Y. Hwang (University of North Texas)
J. Tiley (AFRL/RXLMD)

5d. PROJECT NUMBER
4347

5e. TASK NUMBER
RG

5f. WORK UNIT NUMBER
M02R1000

7. PERFORMING ORGANIZATION NAME(S) AND ADDRESS(ES)
The Ohio State University
University of North Texas
Metals Branch (AFRL/RXLMD)
Metals, Ceramics, and NDE Division
Materials and Manufacturing Directorate
Wright-Patterson Air Force Base, OH 45433-7750
Air Force Materiel Command, United States Air Force

8. PERFORMING ORGANIZATION REPORT NUMBER
AFRL-RX-WP-TP-2008-4327

9. SPONSORING/MONITORING AGENCY NAME(S) AND ADDRESS(ES)
Air Force Research Laboratory
Materials and Manufacturing Directorate
Wright-Patterson Air Force Base, OH 45433-7750
Air Force Materiel Command
United States Air Force

10. SPONSORING/MONITORING AGENCY ACRONYM(S)
AFRL/RXLMD

11. SPONSORING/MONITORING AGENCY REPORT NUMBER(S)
AFRL-RX-WP-TP-2008-4327

12. DISTRIBUTION/AVAILABILITY STATEMENT
Approved for public release; distribution unlimited.

13. SUPPLEMENTARY NOTES
Journal article submitted to *Nature of Materials*. PAO Case Number: WPAFB 08-0489; Clearance Date: 25 Feb 2008. The U.S. Government is joint author of this work and has the right to use, modify, reproduce, release, perform, display, or disclose the work. Paper contains color.

14. ABSTRACT
The high strength of many metallic alloys, including nickel base superalloys used in aircraft jet engines, especially at elevated temperatures, is often attributed to the presence of homogeneously distributed ordered intermetallic precipitates within a disordered matrix. The structure and chemistry at the precipitate/matrix interface plays a critical role in determining the effectiveness of the strengthening mechanism. Combining aberration-corrected high resolution scanning transmission electron microscopy (HRSTEM) with three-dimensional atom probe (3DAP) tomography the atomic scale structure and chemistry across the order/disorder interface in nickel base superalloys has been determined. While, the order/disorder interface is ~4 atomic layers thick, the width of the compositional gradient across the same interface is ~10 atomic layers thick. Such atomic resolution pictures of these interfaces raises fundamental questions regarding their definition and is essential for understanding both their high temperature stability as well as their role in strengthening by obstructing dislocation motion.

15. SUBJECT TERMS
metallic alloys, elevated temperatures, strength, homogeneously distributed ordered intermetallic precipitates, disordered matrix

16. SECURITY CLASSIFICATION OF:			17. LIMITATION OF ABSTRACT:	18. NUMBER OF PAGES	19a. NAME OF RESPONSIBLE PERSON (Monitor)
a. REPORT	b. ABSTRACT	c. THIS PAGE			Christopher F. Woodward
Unclassified	Unclassified	Unclassified	SAR	18	19b. TELEPHONE NUMBER *(Include Area Code)* N/A

Standard Form 298 (Rev. 8-98)
Prescribed by ANSI Std. Z39-18

Direct Atomic Scale Observation of the Structure and Chemistry of Order/Disorder Interfaces

R. Srinivasan, R. Banerjee*, J. Y. Hwang*, G. B. Viswanathan, J. Tiley[#], and, H. L. Fraser

Department of Materials Science and Engineering
The Ohio State University, Columbus, Ohio, U. S. A.

*Department of Materials Science and Engineering
University of North Texas, Denton, Texas, U. S. A.

[#]Materials and Manufacturing Directorate
Air Force Research Laboratory, Dayton, Ohio, U. S. A.

Letter

The high strength of many metallic alloys, including nickel base superalloys used in aircraft jet engines, especially at elevated temperatures, is often attributed to the presence of homogeneously distributed ordered intermetallic precipitates within a disordered matrix[1-2]. The structure and chemistry at the precipitate/matrix interface plays a critical role in determining the effectiveness of the strengthening mechanism[1,3]. Combining aberration-corrected high resolution scanning transmission electron microscopy (HRSTEM) with three-dimensional atom probe (3DAP) tomography the atomic scale structure and chemistry across the order/disorder interface in nickel base superalloys has been determined. While, the order/disorder interface is ~ 4 atomic layers thick, the width of the compositional gradient across the same interface is ~ 10 atomic layers thick. Such atomic resolution pictures of these interfaces raises fundamental questions regarding their definition and is essential for understanding both their high temperature stability as well as their role in strengthening by obstructing dislocation motion.

The present study has been carried out on the Rene88DT commercial nickel base superalloy (with primary alloying elements Al, Ti, Cr, Co, Nb, Mo, and, W), developed specifically for improved performance in turbine disk applications on account of its superior creep and fatigue properties [1,2]. The typical microstructure of Rene88DT consists of a disordered *fcc* γ matrix with ordered $L1_2$ γ' precipitates of varying sizes depending upon processing history [3]. While several studies have discussed the role of precipitate morphology and γ/γ' interface structure and chemistry on the observed mechanical properties [4-6], the limitations associated with the resolution of experimental techniques has typically prevented direct atomic scale imaging of the structure and concurrent measurement of the chemistry across such interfaces. Recent developments in techniques such as 3DAP have enabled detailed exploration of nanometer-scale elemental partitioning across interphase interfaces, including the γ/γ' interface in nickel base

superalloys [7-13]. Furthermore, developments in aberration-corrected HRSTEM now permit imaging and direct interpretation of Z-contrast (arising from the differences in atomic numbers) in atomic resolution images [14-16]. In addition to experimental investigations, a significant amount of research has also focused on modeling of the microstructural evolution [17-19], including atomistic modeling of the γ/γ' interface structure and chemistry [20-23]. This study provides, for the first time, a direct atomic resolution image of the structure and chemistry of the order-disorder γ/γ' interface in a nickel base superalloy by coupling the techniques of 3DAP and aberration-corrected HRSTEM, thus demonstrating the power of combining these two advanced analytical techniques.

An energy-filtered TEM (EFTEM) image, constructed using the Cr M-edge (at 42 eV) in the electron-energy loss spectrum, from the Rene 88DT sample is shown in Fig. 1(a). Details of the procedure used for the EFTEM imaging can be found elsewhere [24]. The morphology and size distribution of γ' precipitates (visible as the darker phase due to Cr depletion) is clearly visible in this image: larger dark features correspond to secondary γ' precipitates, typically formed during cooling from the high temperature (1150°C) single γ phase field, while smaller dark spherical features are the tertiary γ' precipitates formed either during cooling via a second nucleation burst or during ageing at 760°C. Aberration-corrected HRSTEM investigations, using a high angle annular dark-field detector (HAADF), was performed to image the interface between large secondary γ' precipitates and the γ matrix (to ensure a planar interface parallel to the beam direction, across the foil thickness, due to the larger size of these precipitates). Furthermore, for the purpose of maintaining consistency between the HRSTEM and 3DAP analyses, an interface orientation parallel to the (002) planes in γ and γ' phases was specifically chosen. The atomic structure of such an interface (with a beam direction parallel to the <110> *fcc* zone axis) together with the corresponding Fourier transform (inset) are shown in Fig. 1(b) (note the (100) and (110) superlattice reflections from the ordered γ' phase are clearly visible in the Fourier transform). Two filtered sections of the same HRSTEM image, at higher magnifications, with improved image contrast, are shown in Figs. 1(c) and (d). The interface between the γ matrix and the γ' precipitate is clearly visible in these two images. Note that while all the atomic columns exhibit similar intensities in the γ matrix, alternating brighter and darker rows of atomic columns (representative of (002) planes) are observed in the γ' phase. Since this is a HAADF-HRSTEM image, the contrast differences between these atomic columns can be attributed to differences in the average atomic numbers (Z-contrast). The ordered $L1_2$, Ni_3Al-based, structure of the γ' phase consists of two distinct sublattices, the Ni sublattice corresponding to the face-center positions and the Ni+Al mixed sublattice corresponding to the corner positions of the cubic lattice. The presence of these two sublattices leads to (002) planes that consist solely of Ni atoms, alternating with (002) planes that consist of 50% Ni and 50% Al atoms when viewed along any of the <001> type cube axis directions. Even in the case of commercial Ni-base superalloys, such as the alloy under consideration, Rene 88DT consisting of a large number of alloying additions, the γ' phase continues to exhibit the same basic ordering scheme with alternating Ni-rich (with other substitutional atoms) and Al-rich (002) planes. Typically, alloying elements such as Cr and Co segregate to the

disordered γ phase while Ti segregates to the ordered γ' phase in nickel base alloys. Therefore in terms of the Z-contrast in the HAADF-HRSTEM images shown in Fig. 1(b), (c) and, (d), the brighter columns correspond to heavier atoms (such as Ni, Co, Cr) while the relatively darker columns correspond to lighter atoms (such as Al, Ti). The alternating (002) rows of brighter atomic columns and darker atomic columns, clearly visible in the bottom half of the magnified view shown in Fig. 1(d), are direct evidence of the ordered $L1_2$ structure of the γ' phase in this sample and can be referred to as a superlattice contrast. To probe the compositional and structural transition from disordered γ to ordered γ', an intensity profile is plotted across the interface by averaging over the box ABCD (refer to Fig. 1(c)). Such a profile of average intensity versus distance has been plotted in Fig. 2(a), in which the intensity value at a certain distance along the x-axis corresponds to the average of all the atomic columns along a line parallel to AC (or BD) at that distance (note that these lines are parallel to the (002) planes, moving along the [001] direction from AC to BD). The background intensity in the matrix γ phase is expectedly higher, due to the known segregation of heavier alloying elements (such as Cr and Co) to that phase. While the expected superlattice contrast in the γ' phase and lack of it in the γ phase are clearly observed, a definite transition zone is observed at the γ/γ' interface in Fig. 2(a). In order to qualitatively associate the atomic column intensities to site occupancies on the Ni and Ni+Al sublattices, a plot of the intensity ratios of each column to its adjacent column on the right, versus distance, was calculated using the raw intensity values from Fig. 2(a), as shown in Fig. 2(b). The intensity ratios in this plot are a qualitative measure of the site occupancies on the two different sublattices. Thus, for the disordered γ phase this ratio does not change substantially with a value close to 1, since there is no difference in the sublattice occupancies, while in case of the ordered γ' phase the ratio alternates between approximately 1.15 and 0.85 due to the differences in the sublattice occupancies. In Fig. 2(b) moving from the left to the right, as a function of distance, the transition from the γ to the γ' phase is clearly visible with long-range order starting as soon as the value of the intensity ratio changes from ~ 1. Furthermore, there is a clear transition zone at the γ/γ' interface, marked with dotted lines in Figs. 2(b), where the long-range order increases roughly over 4 atomic (002) planes (approximately 0.7 nm). Based on this analysis of Fig. 2(b), the same transition zone has also been marked in the corresponding location in Fig. 2(a). In addition, based on the raw averaged intensities of the atomic columns along the (002) planes shown in Fig. 2(a), there appears to be a transition from the higher intensity columns (higher average Z) on the γ side to the lower intensity columns (lower average Z) on the γ' side. This transition in column intensities can be attributed to a compositional gradient across this interface (also marked with dotted lines in Fig. 2(a)) that is measured to be approximately 1.8 nm in width (or ten (002) planes).

While the aberration-corrected HAADF-HRSTEM study provides a direct Z-contrast atomic resolution image of the order-disorder γ/γ' interface, it is rather difficult to obtain quantitative information regarding the partitioning of alloying elements across this interface as well as the width and extent of the compositional gradient associated with the same interface. 3DAP tomography is an extremely powerful technique for precisely probing such compositional gradients across the γ/γ' interface and has therefore been

employed in this study. The atom probe sample investigated was prepared from the same heat-treated piece of the Rene 88DT alloy that was previously used for the TEM sample preparation. Fig. 3(a) shows a three-dimensional reconstruction of the atom probe sample depicting iso-concentration surfaces for Co (19 at%) in blue and Al (10 at%) in red. Since Co preferentially segregates to the disordered γ phase, the blue regions in Fig. 3(a) correspond to the γ phase while the Al-rich regions in red correspond to the γ' phase. Thus, Fig. 3(a) exhibits a γ channel separating two γ' precipitates. From the size scale of these precipitates it is apparent that these are sections of secondary γ' precipitates. Three-dimensional reconstructions showing only the Al atoms (as black dots) are shown in Figs. 3(b) and (c). In case of Fig. 3(b), as expected the higher concentration of Al atoms lies within the γ' phase and the two γ/γ' interfaces are clearly visible. Fig. 3(c) is a magnified view of the lower γ/γ' interface seen in Fig. 3(b), and clearly shows ordered planes of Al atoms with a plane spacing of approximately 0.36 nm, corresponding to the alternate (002) planes (or (001) planes) in the γ' phase. From Fig. 3(b) it can be concluded that (a) the orientation of the γ/γ' interface is near parallel to the (002) planes in this case and (b) this interface lies near perpendicular to the axis of the atom-probe sample (or the z-axis). It should be noted that Fig. 3(c) exhibits an order-disorder transition zone which is approximately two (001) planes wide (~ 0.7 nm) at the γ/γ' interface. For a statistically relevant quantitative analysis of the compositional gradient across this interface (indicated by an arrow in Fig. 3(d)), compositional profiles for the primary alloying elements have been plotted in the form of a proximity histogram, shown in Fig. 3(d). Based on these profiles, the width of the compositional gradient across the interface (zone separating stable γ and γ' compositions) can be measured to be ~1.8 nm, in excellent agreement with the HRSTEM observations discussed previously.

Recent results on atomistic modeling of the γ/γ' interface in the binary Ni-Al system using an improved inter-atomic potential applied to the Embedded Atom Method by Mishin [22] predict that the order-disorder interface is not atomistically abrupt. In these studies, a grand canonical Monte Carlo simulation was carried out on a supercell containing 1536 atoms and including a coherent γ/γ' interface parallel to the (002) planes. The results of these simulations are shown in Fig. 4 in the form of a plot of Al concentrations, averaged over (002) atomic layers, as a function of distance across the γ/γ' interface. Based on this plot, the decay in long-range chemical order across the interface was predicted to be between 4-6 atomic layers or ~ 0.7 – 1.0 nm. This *predicted* value is in excellent agreement with the experimentally observed width of the order-disorder transition zone at the interface based on the aberration-corrected HRSTEM observations (refer to Figs. 2(a) and (b)). Furthermore, the HRSTEM results coupled with the 3DAP observations indicate significant tolerance to compositional off-stoichiometry within the ordered γ' phase. Referring to the intensity profile shown in Fig. 2(a), the transition zone from γ' to γ is largely accounted for by a progressive increase in the intensity of alternate atomic columns belonging to the Al sublattice, attributable to decreasing Al occupancy (and consequently inceasing Ni occupancy). These observations are again in excellent agreement with the results of Mishin's atomistic simulations which indicate that the off-stoichiometry in the γ' phase occurs by a depletion of Al on the Al sublattice while the Al concentration on the Ni sublattice remains small [22].

Furthermore, modeling studies by Ardell and Ozolins [23] have also indicated the non-abruptness of the γ/γ' interface at elevated temperatures. While the interface width is expectedly higher at temperatures around 1000K, the underlying implications on coarsening and mechanical properties are significant, as has been demonstrated experimentally, for the first time, in this study.

The experimental results presented in this paper not only agree with atomistic simulations and models, but also raise significant questions regarding the basic definition of an order-disorder interface between two phases. Based upon the above results, two different transition zones may be possible for such an interface, one arising from the order-disorder transition, and another one arising due to a compositional gradient. Expectedly, the width of the order-disorder transition is smaller than the compositional gradient in this case, though none of these are atomistically sharp. Such diffuseness in the interface has significant implications on the mechanical properties in Ni-base superalloys as it can potentially influence key parameters such as lattice misfit and coherency between the γ and γ' phases, and subsequent cutting of γ' particles by dislocations. The power of combining the two advanced analytical techniques, outlined in this study, provides a novel way of investigating the interface chemistry and structure in multicomponent systems at the atomic scale.

Methods

Specimens of the Rene88DT alloy, taken from the bore and rim section of a turbine disk (produced and tested under a DARPA program [25]), were subjected to a supersolvus heat treatment (30 mins at 1150^0C), in the single γ phase field, followed by slow cooling at 24^0C/min. Subsequently, the samples were aged for 50 hours at 760^0C, in order to equilibrate the microstructure, resulting in the formation of large (> 200 nm) secondary γ' precipitates (for more details refer [26]). Samples for HRSTEM studies were prepared by conventional methods, including machining of 3 mm discs, followed by ion milling on a Fischione Model 1010 system, and finally completed by nanomilling on a Fischione Model 1040 Nanomill. HRSTEM investigations were conducted on an FEI Titan 80-300 system, operated at 300 kV, equipped with a CEOS electron probe aberration corrector. Needle-shaped 3DAP specimens with a tip radius ~ 50 nm were prepared by a combination of electro-discharge machining (EDM), electropolishing and focused ion beam (FIB) techniques, described in detail elsewhere [24]. 3DAP experiments were conducted on a LEAP 3000 Local Electrode Atom Probe (LEAP^{TM}) microscope system manufactured by Imago Scientific Instruments, Inc.

References

1. R. W. Cahn, *Nature*, **309**, 745 (1984).
2. J. Nutting, *Nature*, **183**, 796 (1959).
3. A. Coujou, M. Benyoucef, M. Legros, and, N. Clement, *Solid State Phenomena*, **60**, 185 (1998).
4. D. D. Krueger, R. D. Kissinger, R. D. Menzies, and, C. S. Wukusick, *U. S. Patent* 4,957,567.
5. D. D. Krueger, R. D. Kissinger, and, R. D. Menzies, *Superalloys 1992*, Ed. S. D. Antolovich et. al., TMS-AIME, Warrendale, PA, 277-286 (1992).
6. S. T. Wlodek, M. Kelly, and, D. A. Alden, *Superalloys 1996*, Ed. R. D. Kissinger, D. J. Deye, D. L. Anton, A. D. Cetel, M. V. Nathal, T. M. Pollock, and, D. A. Woodford, TMS, Warrendale, PA, 129-136 (1996).
7. G.B. Viswanathan, P. Sarosi, M.F. Henry, D.D. Whitis, W.W. Milligan, M.J. Mills, Acta Mater. **53**, 3041- 3057 (2005).
8. J.P. Collier, P.W. Keefe, J.K. Tien, Metall. Trans. A **17**, 651-661 (1986)
9. P.R. Bhowal, E.F. Wright, E.L. Raymond, Metall. Trans. A **21**, 1709-1717 (1990).
10. K.E. Yoon, R.D. Noebe, O.C. Hellman and D.N. Seidman, Surf. Interface Anal. **36**, 594-597 (2004).
11. M.K. Miller, Micron **32**, 757 (2001).
12. K.E. Yoon, D. Isheim, R.D. Noebe and D.N. Seidman, Interface Sci. **9**, 249-255 (2001).
13. D. Blavette, E. Cadel, B. Deconihout, Mater. Charac. **44**, 133-157 (2000).
14. D. Blavette, A. Bostel and J.M. Sarrau, Met. Trans. **16A**, 1703-1711 (1985).
15. A. Buchon, S. Chambreland and D. Blavette, Acta Conf. Du Coll. Nat. Sup. Monoc., Nancy, 129-140 (1990).
16. D. Blavette, L. Letellier, A. Racine and A. Hazotte, MMM, **27**, 185-193 (1996).
17. H. Muller, S. Uhlemann, P. Hartel, M. Haider, Micros. Microanal. **12**, 442-455 (2006).
18. M. Haider, S. Uhlemann, J. Zach, Ultramicroscopy **81**, 163-175, (2000).
19. H. Rose, in *High Res. Imaging and Spectrometry of Materials*, ed. F. Ernst, M. Ruhle, Berlin: Springer-Verlag, 189-270 (2002).
20. I.M. Lifshitz, V.V. Slyozov, J. Phys. Chem. Solids **19**, 35 (1961).
21. C. Wagner, Z. Elektrochem, **65**, 581 (1961).
22. A.J.Ardell, Scripta Metall. Mater. **24**, 343-346 (1990).
23. A.F. Voter, S.P. Chen, Mater. Res. Soc. Symp. Proc. **82**, 175 (1987).
24. Y. Mishin, D. Farkas, M.J. Mehl, D.A. Papaconstantopoulos, Phys. Rev. B **59**, 3393 (1999).
25. Y. Mishin, Acta Mater. **52**, 1451-1467 (2004)
26. A.J. Ardell, V. Ozolins, Nature Materials **4**, 309-316 (2005).
27. J. Hwang, R. Banerjee, J. Tiley, R. Srinivasan, G.B. Viswanathan, H.L. Fraser, submitted to *Met. Trans A* (2008).
28. Defense Advanced Research Projects Agency, Defense Sciences Office (DSO), Engine Systems Prognosis, Contract # HR0011-04-C-0001, HR0011-04-C-0002.
29. J. Tiley, G.B. Viswanathan, R. Srinivasan, R. Banerjee and H.L. Fraser, in

preparation
30. A.A. Hopgood and J.W. Martin, Mater. Sci. Eng. **82**, 27-36 (1986).

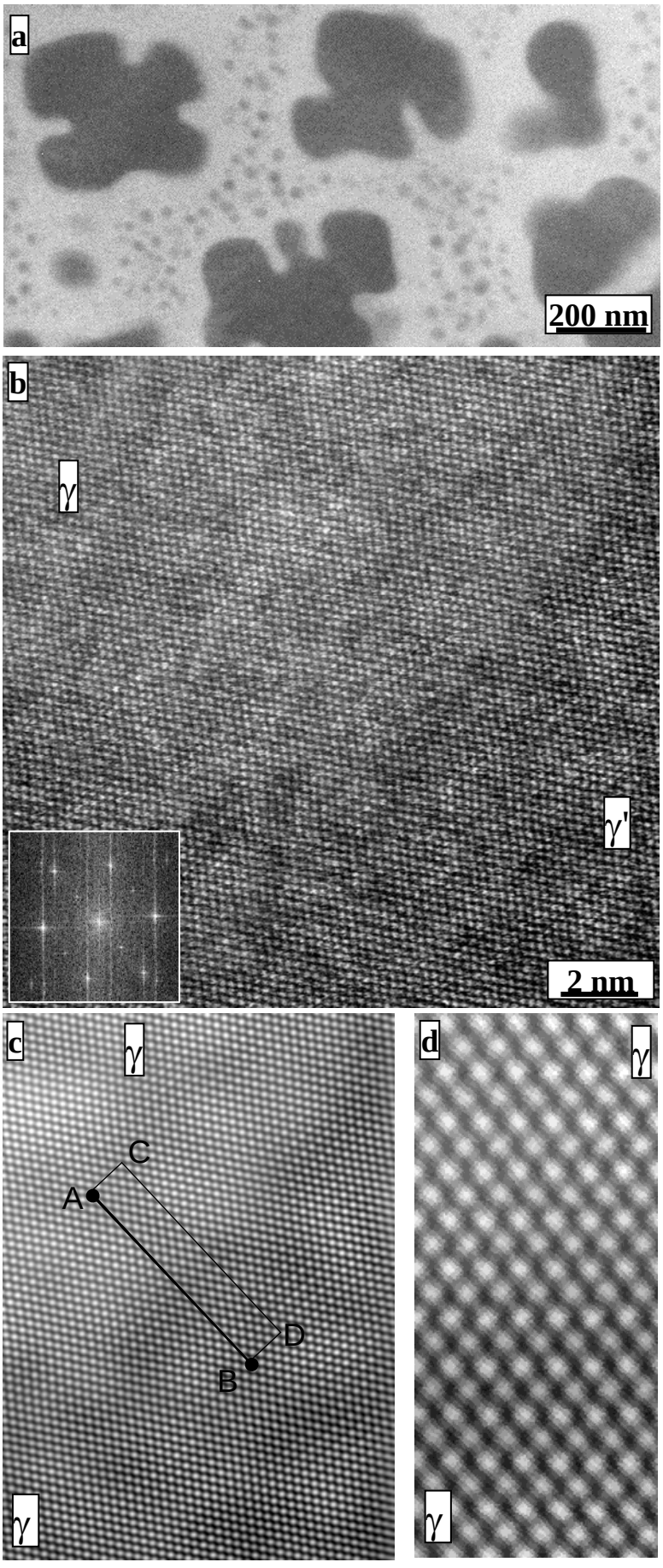
a
200 nm
b
γ
γ'
2 nm
c
γ
C
A
D
B
γ
d
γ
γ

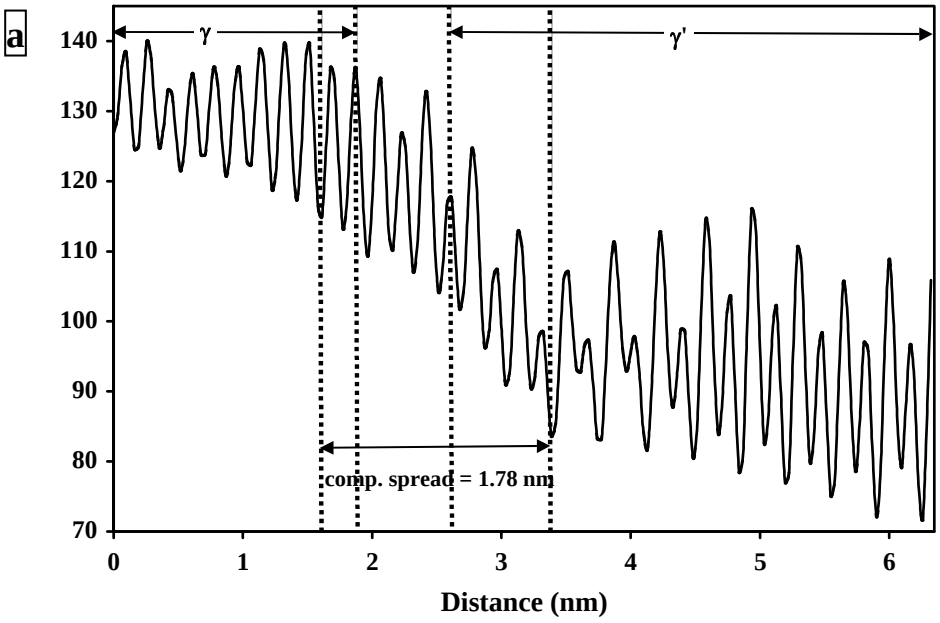
a
γ
γ'
140
130
120
110
100
90
80
70
comp. spread = 1.78 nm
0
1
2
3
4
5
6
Distance (nm)

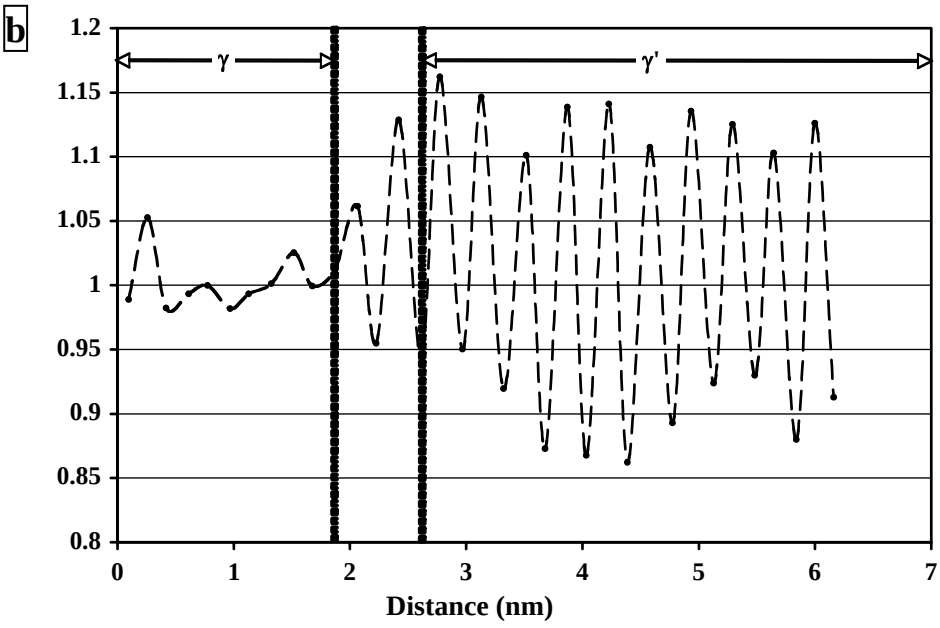
b
γ
γ'
1.2
1.15
1.1
1.05
1
0.95
0.9
0.85
0.8
0
1
2
3
4
5
6
7
Distance (nm)

Fig. 2.

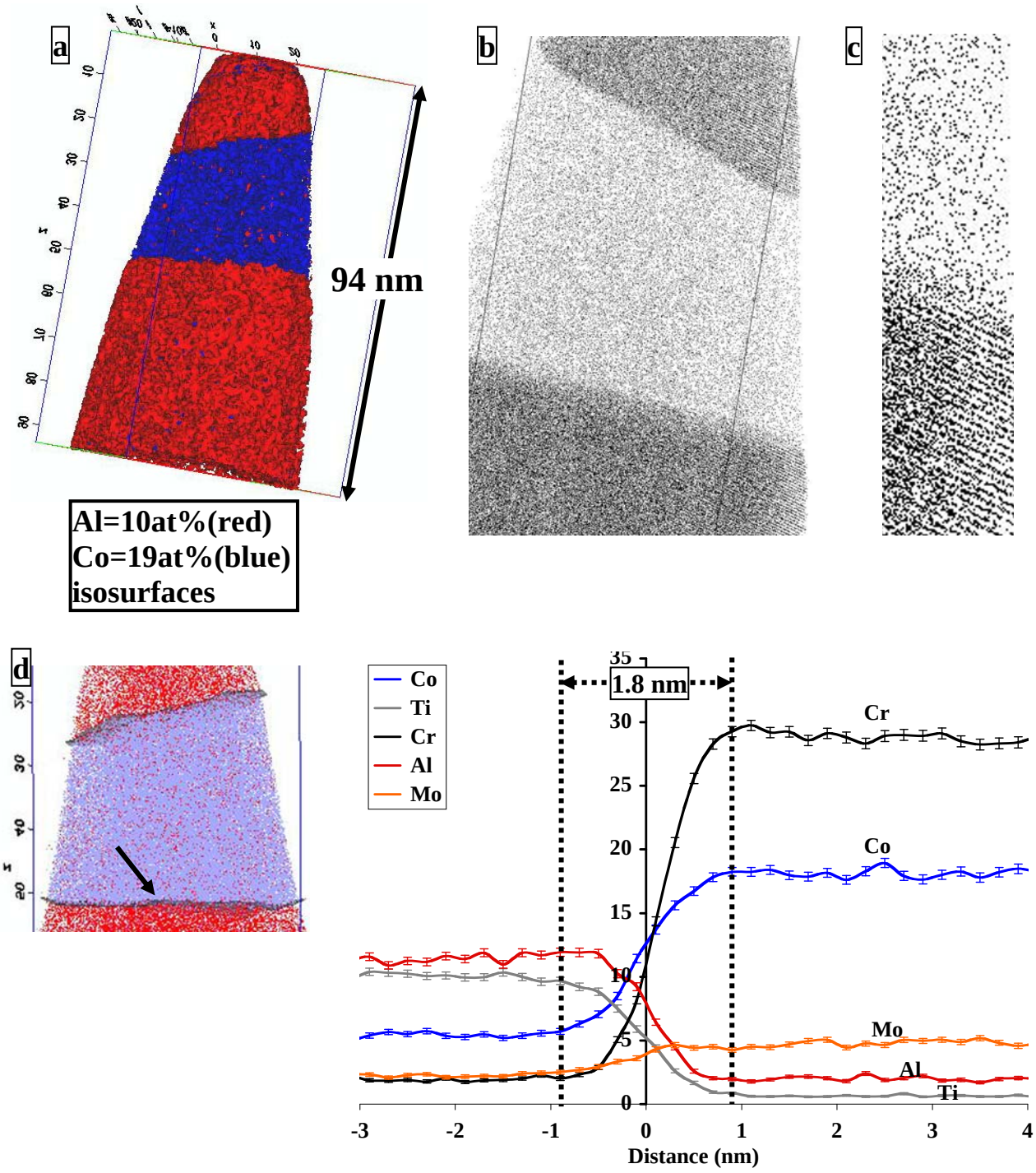
a
94 nm
Al=10at%(red)
Co=19at%(blue)
isosurfaces
b
c
d
Co
Ti
Cr
Al
Mo
1.8 nm
Cr
Co
Mo
Al
Ti
Distance (nm)

Fig. 3.

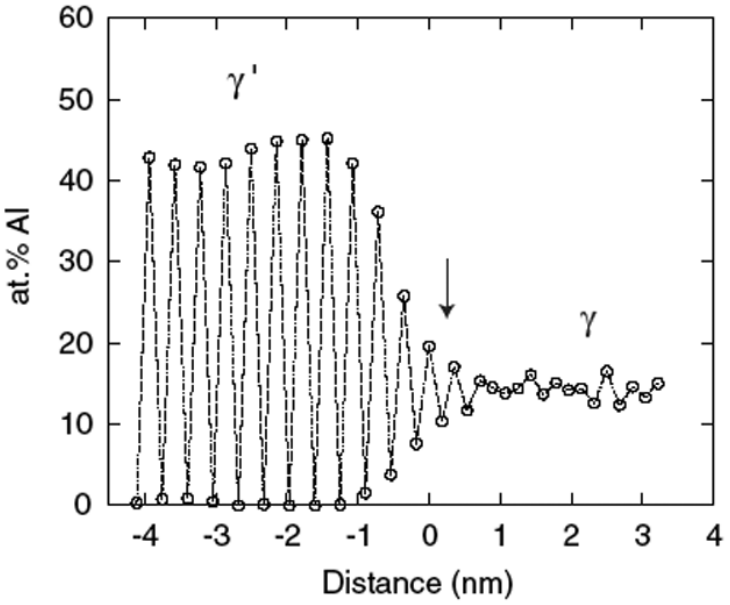

Fig. 4.